Phase stability and interlayer interaction of blue phosphorene

Jeonghwan Ahn, Iuegyun Hong, Yongkyung Kwon, Raymond C. Clay, Luke Shulenburger, Hyeondeok Shin, and Anouar Benali

Phys. Rev. B **98**, 085429 — Published 23 August 2018

DOI: 10.1103/PhysRevB.98.085429

Phase Stability and Interlayer Interaction of Blue Phosphorene

Jeonghwan Ahn, Iuegyun Hong, and Yongkyung Kwon*

Department of Physics, Konkuk University, Seoul 05029, Korea

Raymond C. Clay and Luke Shulenburger

HEDP Theory Department, Sandia National Laboratories, Albuquerque, New Mexico 87185, USA

Hyeondeok Shin

Computational Science Division, Argonne National Laboratory, Argonne, Illinois 60439, USA

Anouar Benali

Computational Science Division, Argonne National Laboratory, Argonne, Illinois 60439, USA and

Leadership Computing Facility, Argonne National Laboratory, Argonne, Illinois 60439, USA

(Dated: July 30, 2018)

Abstract

In this work, we study the interlayer interactions between sheets of blue phosphorus with quantum Monte Carlo (QMC) methods. We find that as previously observed in black phosphorus, interlayer binding of blue phosphorus cannot be described by van der Waals (vdW) interactions alone within the density-functional theory framework. Specifically, while some vdW density functionals produced reasonable binding curves, none of them could provide a correct, even qualitatively, description of charge redistribution due to interlayer binding. We also show that small systematic errors in common practice QMC calculations, such as the choice of optimized geometry and finite-size corrections, are non-negligible given the energy and length scales of this problem. We mitigate some of the major sources of error and report QMC-optimized lattice constant, stacking, and interlayer binding energy for blue phosphorus. It is strongly suggested that these considerations are important and quite general in the modeling of two-dimensional phosphorus allotropes.

PACS numbers: 02.70.Ss, 61.46.-w, 61.50.Lt

*Electronic address: ykwon@konkuk.ac.kr

I. INTRODUCTION

While graphene is arguably the most synthesized and studied two-dimensional (2D) material, the difficulty of opening and tuning a band gap has been a perennial problem, hindering its straightforward application in semiconductor devices. Starting in 2014, there has been a flurry of activity around potentially-realizable 2D layered materials based on phosphorus instead of carbon [1, 2]. Allotropes with layered structures such as black phosphorus, blue phosphorus, and Hittorf's phosphorus are semiconductors with band gaps in the range of 0.3 to 2.5 eV [3–7]. Some allotropes have been successfully synthesized in a single-layer form called phosphorene, such as black phosphorene [1] and more recently blue phosphorene [8, 9].

Given their promise in opto-electronic devices [2], it is essential to understand the underlying physics and energetics of 2D phosphorus layers to a high degree of quantitative accuracy. Being able to accurately predict the energy differences between different mono-layer allotropes informs experimental efforts to determine which allotropes are thermodynamically preferred. Interlayer binding energies are directly related to exfoliation energies, which helps to screen allotropes for ease of mechanical synthesis. Lastly, charge redistribution helps to understand what happens to the electronic properties of a multilayer system as layers are added. We believe that any model capable of simultaneously describing all of these quantities stands a reasonable chance of aiding in the design of phosphorus-based devices in more complicated design spaces, such as by subjecting the layers to stress through the placement on a substrate, or through the addition of defects.

Previous work indicates that at least in black phosphorus, the current generation of van der Waals (vdW) functionals with density-functional theory (DFT) framework does not possess sufficient quantitative accuracy to simultaneously predict relative stability, interlayer binding, and charge redistribution. Benchmarks against fixed-node diffusion Monte Carlo (DMC) and experiment indicate a large spread in the interlayer binding curves [10]. Of the functionals that seem quantitatively predictive on energetic grounds, very few were able to even qualitatively capture the correct charge redistribution. The inconsistency among different density functionals, including vdW-corrected ones, was also pointed out in recent DFT study of Aykol *et al.* on black and red phosphorus [11]. Unfortunately, it is not clear whether the poor performance of vdW density functionals in black phosphorus is intrinsic

to this particular allotrope, or whether 2D phosphorus allotropes generically possess novel physics that the vdW density functionals are systematically failing to capture.

In this paper, we use fixed-node DMC to study the interlayer interactions in a bilayer blue phosphorene. Using the phosphorene geometries optimized directly within DMC, we compute DMC interlayer binding curves for both AA and AB type stackings. When compared against the same binding curves calculated using a variety of different vdW density functionals, we find a similar spread in predicted binding curves as was previously observed in black phosphorus. Moreover, comparison of the fixed-node QMC charge difference between isolated monolayers and the equilibrium bilayer to those calculated within DFT framework suggests that the DFT charge densities are qualitatively and quantitatively incorrect in the same manner as previously observed in black phosphorus. This indicates that the current generation of density functionals are missing some key physics required to quantitatively predict the behavior of phosphorus-based 2D layered materials.

As a secondary concern, we comment on some potential pitfalls to avoid in future quantum Monte Carlo (QMC) work on layered phosphorus materials. While fixed-node DMC is extremely accurate and has the capacity to gracefully handle vdW interaction, covalent bonding, and charge transfer within the same coherent framework, systematic errors that are not intrinsic to the method are often introduced to save computer time. We argue that some common convenience based practices, such as using DFT based structures or using DFT based finite-size corrections, could introduce large errors relative to the energy scales in this problem. We believe this corrects previous QMC calculations which indicated that blue and black phosphorenes are degenerate in energy [12]. We also assess the accuracy of charge densities obtained directly from importance-sampled DMC calculations and find that some quantitative, though not qualitative, differences exist between the DMC estimates and pure estimates derived from reptation Monte Carlo (RMC) calculations.

II. METHODOLOGY

All DFT calculations in this work were done using the QUANTUM ESPRESSO package [13]. We aligned the normal vector of the blue phosphorene layers with the z-axis of our simulation cell. Since QUANTUM ESPRESSO forces periodic boundary conditions, we added a 20 Å vacuum layer along z to minimize spurious interlayer interactions between

periodic images.

We used an LDA based norm-conserving Troullier-Martins [14] pseudopotential with a neon core. Details regarding pseudopotential construction and validation can be found in our previous work [10]. After performing convergence tests, we found that a 250 Ry plane-wave cut off and $12 \times 12 \times 1$ Monkhorst-Pack grid [15] converged the DFT energies to within 3×10^{-10} Ry. We considered the following functionals in this work: LDA [16], PBE [17], PBE+D2 [18], rVV10 [19], TS [20], vdW-DF [21], and vdW-DF2 [22].

All QMC simulations were performed using QMCPACK [23]. The trial wavefunction used in all calculations was the standard Slater-Jastrow type wavefunction. The Jastrow contains short-ranged one- and two-body correlation functions. The one- and two-body functions are expressed using spherically symmetric b-splines, each with a real-space cutoff at the Wigner-Seitz radius of the simulation cell. For the single particle orbitals, we used periodic 3D b-splines fit to the plane wave orbital solutions obtained from QUANTUM ESPRESSO. It was previously established that the lowest variational energies and variances were obtained using the LDA functional [10]. Details of our trial wavefunction can be seen in Ref. 24.

For each geometry considered, we performed the following sequence of QMC calculations. First, all free parameters in the trial wavefunction were optimized with variational Monte Carlo (VMC) using the linear method of Umrigar [25]. Then, DMC was performed with a timestep of $\tau = 0.005$ Ha^{-1} and a population size of 4096 walkers. Unless otherwise specified, imaginary time projection was done with the full non-local Hamiltonian using T-moves [26].

For observables that don't commute with the Hamiltonian, such as the electron density, expectation values taken over the mixed distribution of $\Psi_T \Phi_{FN}$ sampled from DMC can produce a bias of order $\Psi_T - \Phi_{FN}$, where Ψ_T is the trial wavefunction and Φ_{FN} is the fixed node wavefunction. We can combine both VMC and DMC estimates to form "extrapolated estimates" that are accurate to order $(\Psi_T - \Phi_{FN})^2$. In this work, we consider the following two extrapolation formulae: $X_{EXT} = 2X_{DMC} - X_{VMC}$ and $X_{GEO} = (X_{DMC})^2/X_{VMC}$. To benchmark the validity of these extrapolation formulae, we also computed expectation values over $|\Phi_{FN}|^2$ directly on a small selection of geometries. Pure estimates without the trial wave function bias were obtained using RMC [27] as implemented in QMCPACK. For reptation calculations only, propagation was done within the locality approximation. We used reptiles with projection lengths of $\beta = 14$ Ha^{-1} and a time step of $\tau = 0.01$ Ha^{-1}, which was shown

to converge both mixed and pure estimates of the potential energy. We equilibrated 144 reptiles for 1,500,000 time steps. The average acceptance ratio was 98.45%.

Single-particle finite size effects were mitigated using twist-averaged boundary conditions. We considered between 9 twists for the largest supercell and 16 twists for the smallest supercell and used the same variational parameters for different twists of a simulation cell. Residual many-body finite size effects were handled using a standard $1/N$ extrapolation based on 3D homogeneous systems. Supercell sizes of $5 \times 5 \times 1$, $6 \times 6 \times 1$ and $8 \times 8 \times 1$ were used to perform the extrapolation. While the finite-size effects in strictly 2D homogeneous systems are expected to behave like $1/N^{5/4}$, we found a negligible difference in the finite-size extrapolations between the $1/N^{5/4}$ and $1/N$ models, only about 2 meV/atom.

III. RESULTS

A. Optimizing the Monolayer

In order to accurately calculate interlayer binding in blue phosphorus, we need an accurate representation of the monolayer to serve as a reference. For computational convenience, we fixed the P-P bond length to 2.23 Å which is the average of two different bond lengths of black phosphorus [28] and is also within the range of the bond lengths reported in previous DFT studies on blue phosphorene [29–31]. Small variations of the P-P bond length were found to have little effect on our DMC results presented below. In addition, we assume the hexagonal symmetry in optimizing the structure of blue phosphorene because it was predicted in previous DFT studies [32, 33] to be a stable 2D allotrope with a puckered honeycomb structure (see Fig. 1(a)). Due to the hexagonal symmetry of blue phosphorene and the fixed bond length, there is only one free parameter determining the geometry of the monolayer, the lattice constant. Thus to find the lowest energy structure of blue phosphorene, we calculated the fixed-node DMC energies for the aforementioned three supercell sizes with several different lattice constants. The quality of the $1/N$ extrapolation of our supercell energies to the bulk limit can be seen in the Supplemental Material [34]. We show the finite size corrected DMC results in Figure 1. Fitting this curve to Vinet function and finding the minimum, we report the DMC lattice constant of 3.226(2) Å.

Using DMC to calculate the energy of a single phosphorus atom allows us to calculate

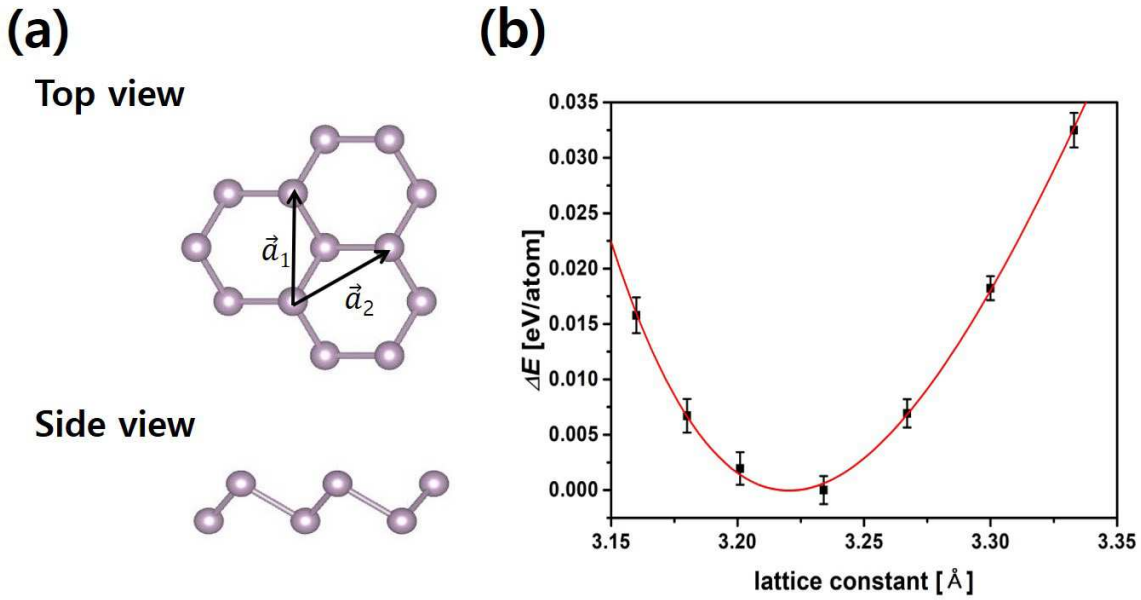

FIG. 1: (Color online) (a) The puckered honeycomb structure of the monolayer blue phosphorene with the hexagonal symmetry ($|\vec{a}_1| = |\vec{a}_2|$) and (b) DMC energy versus lattice constant for blue phosphorene. ΔE is measured relative to the DMC energy of the monolayer with a lattice constant 3.234 Å.

the cohesive energy of blue phosphorene, which we report as 3.272(2) eV/atom. Using the cohesive energies from prior QMC work on black phosphorus [10], we report an energy difference of 32(3) meV/atom between blue and black phosphorene. In Table I, we summarize our findings and compare them to lattice constants, cohesive energies, and relative phase stabilities estimated with LDA and PBE. We note that in contrast to Reeves *et al.*'s relative energies [12], the blue phosphorene has noticeably higher energy than black phosphorene. We discuss the origin of this discrepancy in the last part of this paper.

B. Interlayer Binding Energies

With optimized monolayer geometries in hand, we are now ready to consider the interlayer binding in a blue phosphorene bilayer. Assuming the layers are parallel, we consider two possible stackings: AA and AB. In Figure 2, we present the interlayer binding energy, defined by $\Delta E_{int} = E_{bi}(d) - 2E_{mono}$, as a function of interlayer separation d for both stackings. After fitting the binding curves to Morse potentials (see the solid lines in Fig. 2), we can extract

	PBE	LDA	DMC
Lattice constant (Å)	3.279	3.201	3.226(2)
Cohesive energy (eV/atom)	3.465	4.329	3.272(2)
$\Delta E = E_{blue} - E_{black}$ (eV/atom)	0.005	0.027	0.032(3)

TABLE I: Equilibrated lattice constants and cohesive energies of blue phosphorene, along with the energy differences between black and blue phosphorenes (ΔE), which were estimated with LDA, PBE and DMC calculations.

the following equilibrium binding energies: 40(1) meV/atom and 29(1) meV/atom for the AA and AB stackings respectively. We find the equilibrium interlayer separations for the AA and AB stackings to be 4.84(2) Å and 5.34(2) Å, respectively. Thus, fixed-node DMC predicts the AA stacking to be energetically preferable to AB by about 11(2) meV/atom, which is geometrically reflected in the significantly reduced equilibrium interlayer spacing.

We now consider how well interlayer binding versus interlayer separation is described using different vdW functionals within the DFT framework. In Figure 3, we overlay the interlayer binding curves for PBE+D2, TS, rVV10, vdW-DF and vdW-DF2 on top of our calculated DMC binding curves. To the left we show the results for the AA stacking, and to the right the ones for the AB stacking. Qualitatively, all functionals agree on the binding behavior and relative stabilities of AA vs AB. Quantitatively, the span in binding energies is approximately 30 meV/atom, whereas the span in interlayer distances is approximately 0.4 Å. We summarize the equilibrium binding energies and interlayer distances in Table II. The two most accurate functionals we identify are rVV10 and vdW-DF2. rVV10 has the closest agreement with DMC regarding the absolute binding energies for the AA and AB phases, whereas vdW-DF2 more accurately predicts the equilibrium interlayer separation.

C. Charge Transfer

Up to now, we've looked at interlayer binding from a purely energetic perspective. Now we turn our attention to how the electrons are redistributing themselves in the bilayer as a result of electronic correlations. To accomplish this, we begin by computing the electron charge density of the monolayer $\rho_0(\mathbf{r})$. Then we compute the charge density of a bilayer

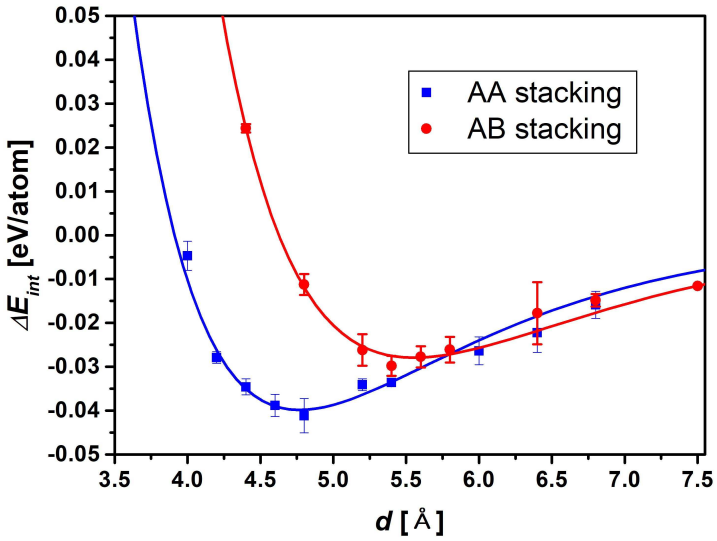

FIG. 2: (Color online) DMC interlayer binding energy ΔE_{int} versus interlayer separation d. In the dissociated limit, $\Delta E_{int}(d \to \infty) = 0$.

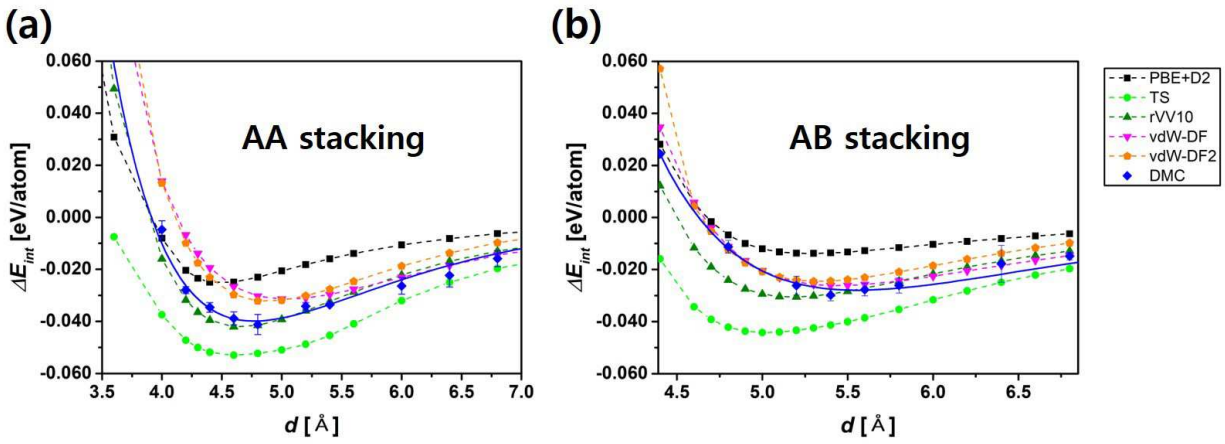

FIG. 3: (Color online) Interlayer binding energy curves of (a) AA- and (b) AB-stacked bilayer blue phosphorenes as functions of interlayer distance.

with AA stacking $\rho_{bi}(\mathbf{r})$ at equilibrium. The charge transfer $\Delta\rho(\mathbf{r})$ is computed by looking at the difference between the bilayer charge distribution and the sum of the charges from the two monolayers located at the corresponding positions of its bilayer form: $\Delta\rho(\mathbf{r}) = \rho_{bi}(\mathbf{r}) - (\rho_0^{upper}(\mathbf{r}) + \rho_0^{lower}(\mathbf{r}))$. To simplify the analysis, we integrate out the x and y dependence of $\Delta\rho(\mathbf{r})$ by averaging the charge difference over x and y, leaving $\Delta\rho(z)$.

Method	AA stacking		AB stacking	
	E_b (eV/atom)	d_{eq} (Å)	E_b (eV/atom)	d_{eq} (Å)
PBE+D2	0.024	4.61	0.014	5.33
TS	0.054	4.58	0.044	5.06
rVV10	0.041	4.70	0.031	5.21
vdW-DF	0.032	5.06	0.026	5.46
vdW-DF2	0.032	4.93	0.025	5.33
DMC	0.040(1)	4.84(2)	0.029(1)	5.34(2)

TABLE II: DMC and DFT equilibrium interlayer binding energies (E_b) and distances (d_{eq}) in AA- and AB-stacked bilayer blue phosphorenes.

In Figure 4, we compare the charge redistribution $\Delta\rho(z)$ predicted by several different functionals against RMC. While RMC and the various density functionals roughly agree on the scale of charge redistribution, there are subtle quantitative and qualitative disagreements between all the functionals and RMC. RMC predicts a sharp charge accumulation on the interior surfaces of the bilayer and an accumulation of charge on the external surfaces, which is compensated by strong charge depletion both in the interior of the bilayer and within each monolayer. This charge redistribution in the bilayer can be understood by the interlayer electron-electron correlation that tends to push lone pair electrons in the interior toward the inner surface of their affiliated layer and subsequently induces the migration of charge within the monolayers to the exterior. The only vdW functional that even comes close to reproducing this picture is vdW-DF2, which does so only qualitatively and only in the interior region between the monolayers. In contrast to the RMC results, all functionals including vdW-DF2 predict weak charge depletion on the exterior of the bilayer. Within the monolayers themselves, all functionals predict weak charge accumulation and depletion as one goes from the exterior to the interior of the bilayer. We also estimated the change of the total charge in each region, by integrating the charge density differences of Figure 4 over the interior, the exterior, and the monolayer regions. While RMC showed a net charge transfer from the monolayer to the exterior with little change in the total charge of the interior region, all DFT results showed no significant charge transfer between different regions. This

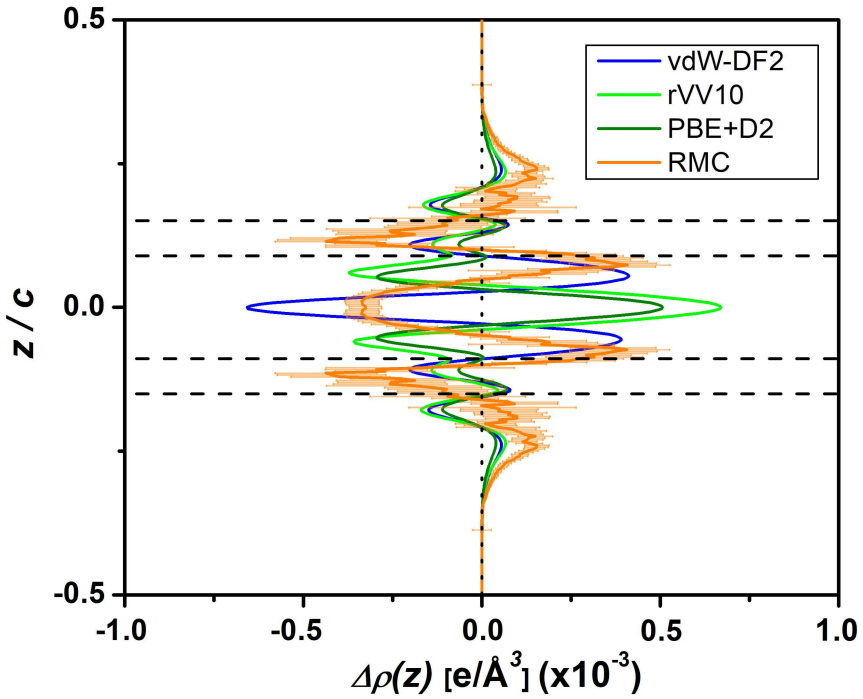

FIG. 4: (Color online) Charge density differences computed by vdW-corrected DFT as well as by the RMC pure estimator for an AA-stacked bilayer blue phosphorene at the equilibrium interlayer distance. The RMC computations were done with the $2 \times 2 \times 1$ supercell. A horizontal dashed line represents each relative coordinate of the phosphorus plane where the adjacent lines stand for a single-layer blue phosphorene. The vertical dotted line represent the one for the zero density. The RMC data were symmetrized with respect to $z = 0$ to reduce statistical noises that are represented by thin orange lines.

suggests that changes in electronic properties of a bilayer blue phosphorene compared to those of its monolayer form, such as band gap reduction [6, 29], could be underestimated in DFT calculations.

In order to understand the effects of charge redistributions on the electronic properties of a bilayer blue phosphorene, we performed non-self-consistent PBE calculations based on both PBE+D2 and vdW-DF2 charge densities [35]. While the binding energy scale due to charge redistribution was found to be much smaller than the vdW energy scale, the PBE band gaps computed with these two charge densities differed from each other by 0.29 eV. This suggests that smalll errors in the treatment of the interlayer vdW interaction could lead to qualitatively different charge redistributions and so noticeably different electronic

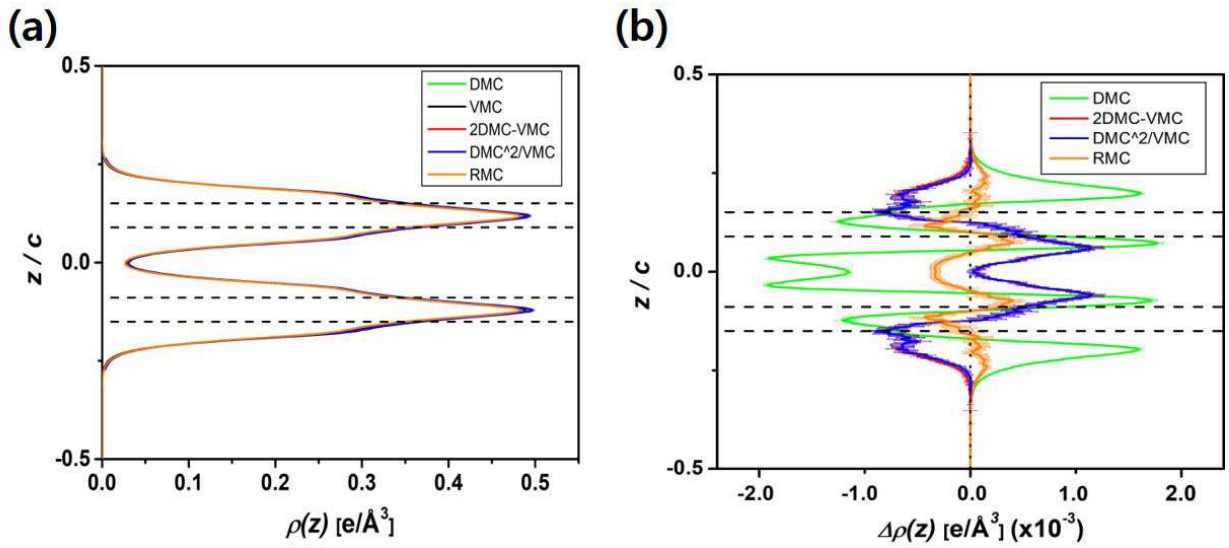

FIG. 5: (a) $\rho(z)$ for the bilayer computed with VMC, the DMC mixed-estimate, and two extrapolated estimators, along with RMC pure estimate (b) $\Delta\rho(z)$ computed using DMC, two extrapolated estimates, and RMC. All QMC data in (b) were symmetrized with respect to $z = 0$ to reduce statistical noises that are represented by thin lines.

structures of a bilayer blue phosphorene. Therefore one can say that an accurate description of both interlayer binding energy and charge redistribution is essential for comprehensive understanding of the vdW interaction of blue phosphorus.

D. Computational Pitfalls

In this section, we pause to discuss some potential pitfalls that we discovered during this work that necessarily must be accounted for in future QMC-based calculations on layered phosphorus allotropes. The first point is the importance of using QMC optimized geometries, and the second is the potentially substantial quantitative inaccuracy of mixed estimators for charge density distributions relative to pure estimates.

We note that our current estimates for the relative stability of blue phosphorene disagree with the QMC work of Reeves *et al.* [12]. We predicted in section III that a blue phosphorene is 32(3) meV/atom higher in energy than a black phosphorene, whereas Reeves *et al.* predicted that black and blue phosphorenes were degenerate within their DMC error bars.

While there are many ways for subtle errors to creep into a DMC calculation, such

as choice of pseudopotential, single-particle orbitals, ground-state structure, and choice of finite-size corrections, a direct comparison of our work to theirs allows us to comment on the sizes of the ground-state structure errors and finite size corrections. Using the DMC blue phosphorene equation of state in Figure 1 and the black phosphorene equation of state from Shulenburger *et al.*, we find that using the PBE lattice constants instead of the DMC optimized lattice constants underestimates the DMC cohesive energies of blue and black phosphorenes by 10 meV/atom and 15 meV/atom, respectively. Thus, these errors lower the relative energy difference between blue and black phosphorenes by about 5 meV/atom. Moreover, Reeves *et al.* found that the error incurred using LDA based KZK [36] finite size corrections was approximately 7 meV/atom relative to the $1/N$-based extrapolation. The sizes of these errors are large when compared against the relevant energy scales in this problem. To put this in perspective, half of all tested functionals give binding energies for AA and AB stacking of blue phosphorene within 10 meV/atom of DMC. While a total resolution of this discrepancy is probably not possible without a direct comparison of pseudopotentials, single-particle orbitals, time-step extrapolations, etc., we find it unlikely that the claim that blue and black phosphorenes are isoenergetic within DMC will hold up when the sources of error discussed in this section are removed.

Secondly, we discuss the potential pitfalls of using DMC mixed or extrapolated density estimates in layered phosphorus. In Figure 5, we plot the charge density distributions of a bilayer blue phosphorene averaged over x and y coordinates, $\rho(z)$, which were calculated using VMC, DMC mixed, and two extrapolated estimators, along with RMC pure estimator. We find that they are all nearly indistinguishable from each other, implying that there is no major breakdown or disagreement in the charge density between the different levels of theory. However, in blue phosphorus and other layered allotropes, the relevant physics is described by $\Delta\rho(z)$, which is roughly 1,000 times smaller in magnitude than $\rho(z)$. On this scale, we find that the trial function bias in DMC mixed density estimate is quantitatively significant. The RMC charge transfer maxima in Figure 5 are roughly 0.0005 e/Å^{-3}, whereas the charge transfer scale for DMC mixed estimates is roughly 0.002 e/Å^{-3}, about a factor of 4 off of the correct answer. For the extrapolated estimates, while the charge transfer scale is much closer to that of RMC than the original mixed estimates, there are noticeable qualitative differences relative to both RMC and the mixed estimates; RMC and DMC mixed estimates predict charge depletions at the center of the bilayer along with charge

accumulations on the interior and exterior surfaces, whereas the extrapolated estimates show charge depletion on the exterior and net charge accumulation in the interior without charge depletion at its center. This strongly suggests that forward-walking or RMC is a requirement for resolving the charge redistribution scales in layered phosphorus allotropes while providing its qualitatively correct picture, unless trial wave functions are of high quality.

IV. CONCLUSION

From an analysis of DMC bilayer binding curves with two different stackings and from RMC estimates of the charge redistribution, we have found that currently-available vdW functionals do not provide a correct description of the interlayer binding of blue phosphorene, both in energy and in charge redistribution, within the DFT framework. There is some subtle but non-negligible charge redistribution occurring over very small length scales. The importance of both vdW interaction and charge redistribution makes the current generation of vdW functionals largely incapable of simultaneously describing multiple properties accurately. For instance, the most accurate interlayer binding energies are given by rVV10, whereas the most accurate interlayer binding distances are given by vdW-DF2. When it comes to charge redistribution, no vdW-corrected functional considered in this study is qualitatively accurate in all of space, although vdW-DF2 does a reasonable job describing charge redistribution within the interior of the bilayer.

Due to the observed presence of strong charge localization and redistribution in the bilayer, one potential area for improvement in DFT based calculations for layered phosphorus allotropes might be in using new classes of non-local vdW hybrid functionals [37]. It is known that self-interaction error in DFT is likely to favor smoother, more delocalized charge distributions, which would tend to discourage charge transfer from one region to another in the formation of a bilayer. We think that mitigating this source of error, in addition to properly describing non-local vdW interactions, is likely to allow DFT to provide a more equitable and accurate description of multiple properties simultaneously and over larger regions of space.

Acknowledgments

This work was supported by Konkuk University 2014. We also acknowledge the support from the Supercomputing Center/Korea Institute of Science and Technology Information with supercomputing resources including technical support (KSC-2016-C3-001).

AB, RCC, HS and LS were supported by the U.S. Department of Energy, Office of Science, Basic Energy Sciences, Materials Sciences and Engineering Division, as part of the Computational Materials Sciences Program and Center for Predictive Simulation of Functional Materials.

Sandia National Laboratories is a multimission laboratory managed and operated by National Technology & Engineering Solutions of Sandia, LLC, a wholly owned subsidiary of Honeywell International Inc., for the U.S. Department of Energys National Nuclear Security Administration under contract DE-NA0003525.

---

[1] H. Liu, A. T. Neal, Z. Zhu, Z. Luo, X. Xu, D. Tománek, and P. D. Ye, ACS nano **8**, 4033 (2014).

[2] L. Li, Y. Yu, G. J. Ye, Q. Ge, X. Ou, H. Wu, D. Feng, X. H. Chen, and Y. Zhang, Nature Nanotech. **9**, 372 (2014).

[3] L. Li, J. Kim, C. Jin, G. J. Ye, D. Y. Qiu, H. Felipe, Z. Shi, L. Chen, Z. Zhang, F. Yang, et al., Nature Nanotech. **12**, 21 (2017).

[4] V. Tran, R. Soklaski, Y. Liang, and L. Yang, Phys. Rev. B **89**, 235319 (2014).

[5] J.-H. Choi, P. Cui, H. Lan, and Z. Zhang, Phys. Rev. Lett. **115**, 066403 (2015).

[6] J. Guan, Z. Zhu, and D. Tománek, Phys. Rev. Lett. **113**, 046804 (2014).

[7] G. Schusteritsch, M. Uhrin, and C. J. Pickard, Nano Lett. **16**, 2975 (2016).

[8] J. L. Zhang, S. Zhao, C. Han, Z. Wang, S. Zhong, S. Sun, R. Guo, X. Zhou, C. D. Gu, K. D. Yuan, et al., Nano Lett. **16**, 4903 (2016).

[9] C. Gu, S. Zhao, J. L. Zhang, S. Sun, K. Yuan, Z. Hu, C. Han, Z. Ma, L. Wang, F. Huo, et al., ACS nano **11**, 4943 (2017).

[10] L. Shulenburger, A. D. Baczewski, Z. Zhu, J. Guan, and D. Tomanek, Nano Lett. **15**, 8170 (2015).

[11] M. Aykol, J. W. Doak, and C. Wolverton, Phys. Rev. B **95**, 214115 (2017).

[12] K. G. Reeves, Y. Yao, and Y. Kanai, J. Chem. Phys. **145**, 124705 (2016).

[13] P. Giannozzi, S. Baroni, N. Bonini, M. Calandra, R. Car, C. Cavazzoni, D. Ceresoli, G. L. Chiarotti, M. Cococcioni, I. Dabo, et al., J. Phys.: Condens. Matter **21**, 395502 (2009).

[14] N. Troullier and J. L. Martins, Phys. Rev. B **43**, 1993 (1991).

[15] H. J. Monkhorst and J. D. Pack, Phys. Rev. B **13**, 5188 (1976).

[16] J. P. Perdew and A. Zunger, Phys. Rev. B **23**, 5048 (1981).

[17] J. P. Perdew, K. Burke, and M. Ernzerhof, Phys. Rev. Lett. **77**, 3865 (1996).

[18] S. Grimme, J. Antony, S. Ehrlich, and H. Krieg, J. Chem. Phys. **132**, 154104 (2010).

[19] R. Sabatini, T. Gorni, and S. de Gironcoli, Phys. Rev. B **87**, 041108 (2013).

[20] A. Tkatchenko and M. Scheffler, Phys. Rev. Lett. **102**, 073005 (2009).

[21] M. Dion, H. Rydberg, E. Schröder, D. C. Langreth, and B. I. Lundqvist, Phys. Rev. Lett. **92**, 246401 (2004).

[22] K. Lee, É. D. Murray, L. Kong, B. I. Lundqvist, and D. C. Langreth, Phys. Rev. B **82**, 081101 (2010).

[23] J. Kim, K. P. Esler, J. McMinis, M. A. Morales, B. K. Clark, L. Shulenburger, and D. M. Ceperley, **402**, 012008 (2012).

[24] J. Kim, A. T. Baczewski, T. D. Beaudet, A. Benali, M. C. Bennett, M. A. Berrill, N. S. Blunt, E. J. L. Borda, M. Casula, D. M. Ceperley, et al., J. Phys.: Condens. Matter **30**, 195901 (2018).

[25] C. J. Umrigar, J. Toulouse, C. Filippi, S. Sorella, and R. G. Hennig, Phys. Rev. Lett. **98**, 110201 (2007).

[26] M. Casula, Phys. Rev. B **74**, 161102 (2006).

[27] S. Baroni and S. Moroni, Phys. Rev. Lett. **82**, 4745 (1999).

[28] A. Brown and S. Rundqvist, Acta Cryst. **19**, 684 (1965).

[29] B. Ghosh, S. Nahas, S. Bhowmick, and A. Agarwal, Phys. Rev. B **91**, 115433 (2015).

[30] J.-J. Zhang and S. Dong, 2D Mat. **3**, 035006 (2016).

[31] C. Chowdhury, S. Jahiruddin, and A. Datta, J. Chem. Phys. Lett. **7**, 1288 (2016).

[32] S. E. Boulfelfel, G. Seifert, Y. Grin, and S. Leoni, Phys. Rev. B **85**, 014110 (2012).

[33] Z. Zhu and D. Tománek, Phys. Rev. Lett. **112**, 176802 (2014).

[34] See Supplemental Material at [*URL will be inserted by publisher*] for the details of the $1/N$

extrapolation of the DMC supercell energies to the bulk limit.

[35] Because we cannot distinguish the binding energy contribution of charge redistribution from that of the vdW interaction with QMC calculations, DFT calculations are used to analyze effects of charge redistribution.

[36] H. Kwee, S. Zhang, and H. Krakauer, Phys. Rev. Lett. **100**, 126404 (2008).

[37] K. Berland, Y. Jiao, J.-H. Lee, T. Rangel, J. B. Neaton, and P. Hyldgaard, J. Chem. Phys. **146**, 234106 (2017).